Supporting Information

A Retinomorphic Neuron for Artificial Vision and Iris Accommodation

Lin Sun, Shangda Qu, and Wentao Xu*

Institute of Photoelectronic Thin Film Devices and Technology, Key Laboratory of Photoelectronic Thin Film Devices and Technology of Tianjin, College of Electronic Information and Optical Engineering, Engineering Research Center of Thin Film Photoelectronic Technology of Ministry of Education, Smart Sensing Interdisciplinary Science Center, Nankai University, Tianjin 300350, China

Shenzhen Research Institute of Nankai University, Shenzhen 518000, China

E-mail: wentao@nankai.edu.cn

Table of contents:

Experimental Section/Methods

Fabrication and measurement of Au modified ITO fiber photonic synapse

Poly(vinylpyrrolidone) (PVP, Mw = 1300,000 g mol^{-1}, Rhawn) was used as a sacrificial polymer, Stannous chloride dihydrate (SnCl$_2$·2H$_2$O, 98%, Innochem) and Indium nitrate hydrate (In(NO$_3$)$_3$·xH$_2$O, 99.9%, Innochem) were used as metallic precursors. They were dissolved in *N,N*-Dimethylformamide (DMF, 99.8%, Meryer) and stirred at 50 °C overnight. A homemade electrohydrodynamic printer was used to print a controlled arrangement of hybrid fibers made of sacrificial polymers and precursors. After the printing process, the product is calcined in a tube furnace at approximately 500 °C for 2 h before growth of Au NPs. The Au NPs were modified by reduction method of hydrated gold hypochlorite. Then 100 nm of Au was deposited/evaporated on to the patterns by using thermal evaporation. The Au NP aqueous solution was purchased from XFNANO as reference samples.

Fabrication of sandwich-type electrochromic device

The sandwich-type electrochromic device was composed of ITO/PET substrates, electrochromic layer that used PEDOT: PSS, and gel electrolyte layer that used LiClO$_4$. Electrochromic ink that used PEDOT: PSS (CHRO-EP202-P) and LiClO$_4$ electrolyte (ENER-EI30M) were purchased from Shanghai Mifang Electronic Technology co. LTD. The electrochromic device was prepared according to the following steps. First, the ITO/PET substrates were treated with UV-ozone for 15 min. The electrochromic ink was spin-coated (1500 rpm, 30 s) on ITO/PET substrate and then annealed at 120 °C for 30 min. The gel electrolyte was spread on another ITO/PET substrate by using an applicator. Finally, the ITO/PET substrates were assembled to form a sandwich-type electrochromic device.

The Kelvin probe force microscopy (KPFM) and atomic force microscopy (AFM) images were recorded on a Bruker Multimode 8 system equipped with Pt/Ir coated tips and NanoScope V controller. The crystal structure of sample was characterized by powder X-ray Diffraction (XRD) (Rigaku Ultima IV). X-ray photoelectron spectra (XPS) were obtained using an ESCALAB 250Xi electron spectrometer (Thermo Fisher Scientific Corporation). The transmittance spectrum was conducted on the AGILENT Cary 5000 UV-vis-NIR spectrophotometer. Electrical measurements were performed at room temperature using a Keithley 4200A semiconductor parameter analyzer. Monochromatic light was obtained using a 150 W xenon lamp configured with a

monochromator. Calibrate the optical power using a standard silicon optical power meter.

Construction of artificial iris vision system

Here, we mimic the visual afferent nerves and neural communication by integrating our artificial synapses with a light-dependent sensor by a multi-vibrator circuit (Figure S9). The design of the sensing-oscillator circuit part can be found in our previous work on artificial reflex arcs [47]. Encoding stimulus information by pulse frequency in the artificial retinomorphic neuron. Here, we mimic the visual neural communication by integrating our artificial synapses with a sensor (light-dependent neuromorphic photoreceptors) by an improving multi-vibrator circuit (Figure S9). Commercially available electronic components (2 capacitors, 1 resistor, 2 diodes, 1 555- timer chip) were used to ensure the operational stability of the system. Here the neuromorphic photoreceptor device acts as a variable photoresistor, and the resistance value affects the frequency of the generated electrical pulses. The frequency of electrical pulses could be increased when stimulated by stronger light or elongated illumination time, and then tune the color of the electrochromic device to act as an artificial iris, which controlled light flux. For simulating direct and consistent pupillary light reflexes. we integrate two electrochromic devices through a parallel circuit to form a pair of irises. When the light source is near the artificial photoreceptor, the change in the resistance value causes the frequency output of the oscillating unit, and the appropriate amplitude of the electrical spikes will drive both color-changing devices at the same time. When we stimulate the artificial receptors on one side, a pair of artificial irises will work simultaneously.

I. Anatomy of the light reflex

Anatomy of the sympathetic pathway: Begins with the first-order neuron, which originates in the hypothalamus and travels down the spine, synapsing onto the ciliospinal center of Budge. The second-order neuron then projects from the ciliospinal center of Budge, then travels upwards over the apex of the lung and terminates onto the superior cervical ganglion located in the neck. Information is then passed onto the third order neuron, which sends its projections from the superior cervical ganglion along the internal carotid artery through the cavernous sinus, joining the ophthalmic portion of the trigeminal nerve and eventually reaching the ciliary body and the dilator muscle of the pupil.

Parasympathetic pathway: Response to light is mediated by the retinal photoreceptors that conduct the signal to the pretectal nucleus. Fibers from the nasal retina cross over in the chiasm and enter the nasal retina do not decussate and send information to the ipsilateral pretectal nucleus in the midbrain. Input from the pretectal nuclei is then transmitted to the Edinger-Westphal (EW) nuclei. Information from the ipsilateral pretectal nucleus relays information to both the contralateral and ipsilateral EW nuclei, thus explaining why light stimulation of one eye causes equal and symmetrical pupil constriction of the other eye. Neurons then leave the EW nucleus and synapse onto the ipsilateral ciliary ganglion. Fibers from the ciliary ganglion pass through the short ciliary nerves, causing innervation of the ipsilateral pupil sphincter.
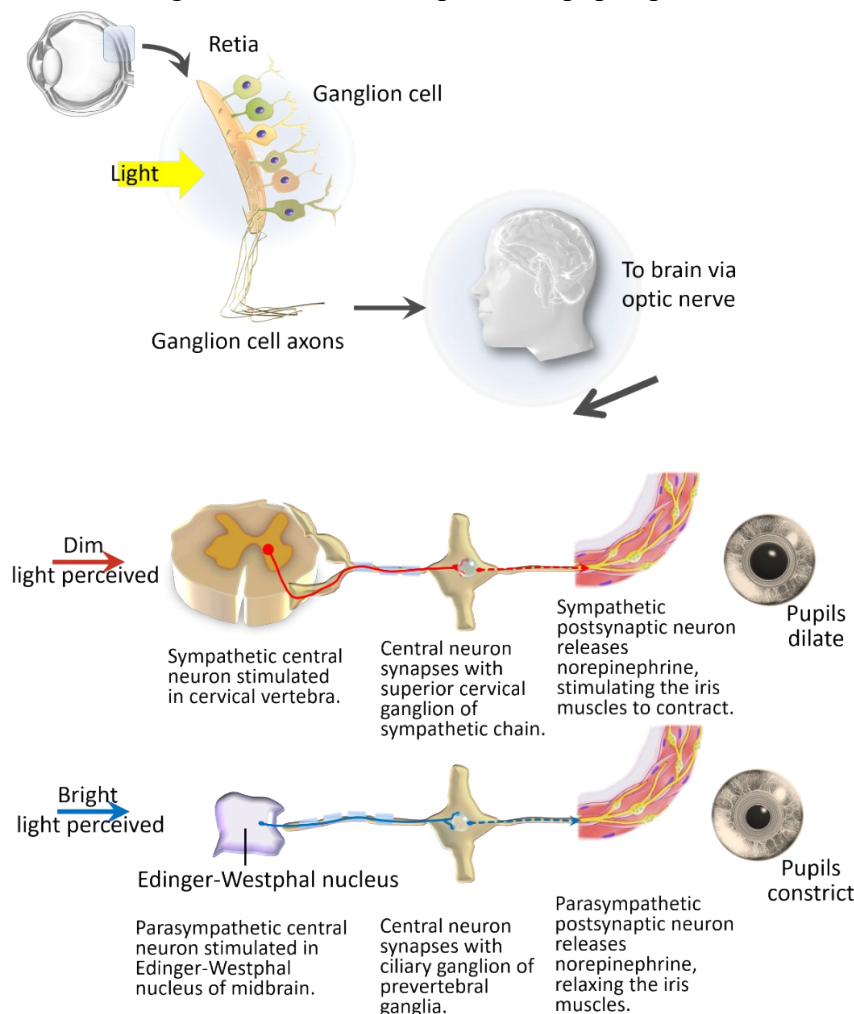

Figure S1. Pupillary reflex and accommodation. Autonomic control of pupil size.

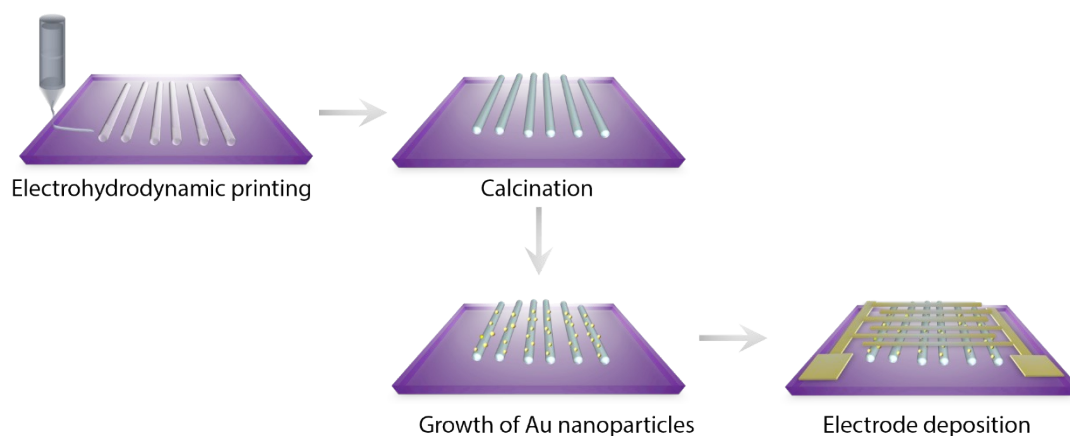## II. Fabrication and characterization of fiber photonic synapse

Electrohydrodynamic printing → Calcination

Growth of Au nanoparticles → Electrode deposition

Figure S2 Schematic illustration of the process to fabricate aligned ITO/Au photonic synapse.

80 µm

500 nm
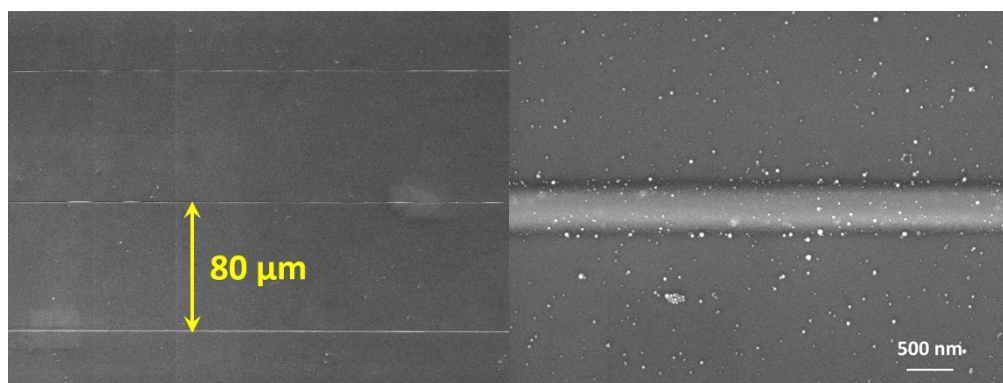
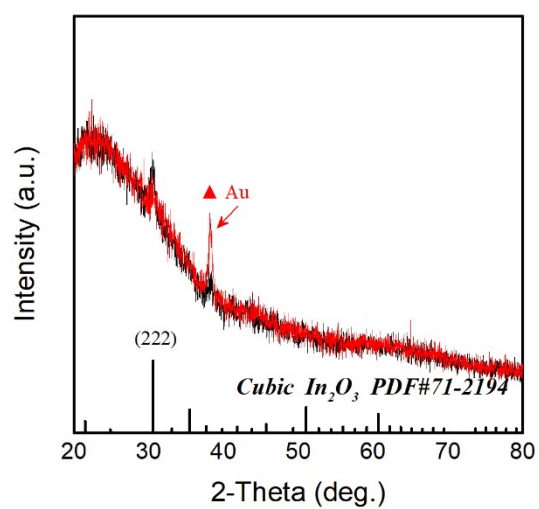Figure S3. SEM images of fabricated Au-ITO fibers.

Intensity (a.u.)

▲ Au

(222)

Cubic In_2O_3 PDF#71-2194

2-Theta (deg.)

Figure S4. XRD pattern of fabricated Au-ITO fiber.
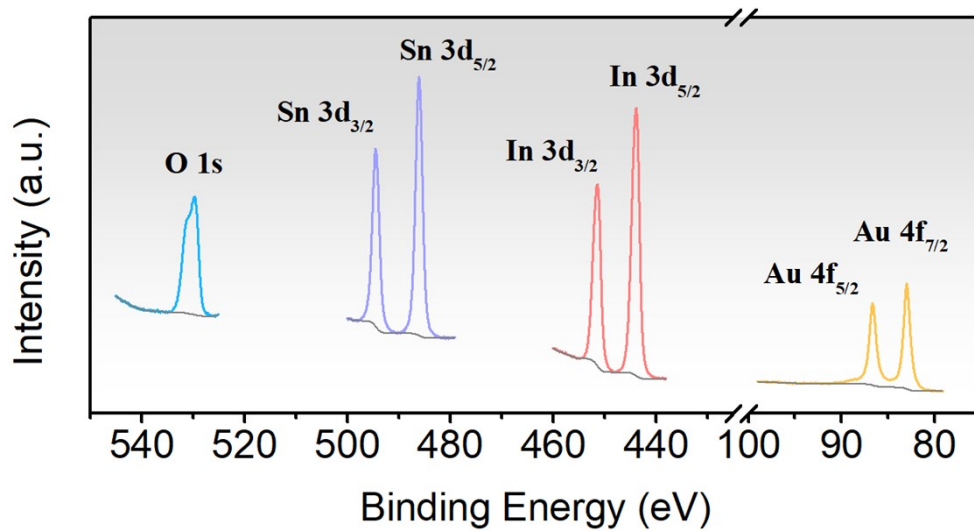
Figure S5. XPS spectrum of Au-ITO, and corresponding regional peaks of O 1s, Sn 3d, In 3d, Au 4f.

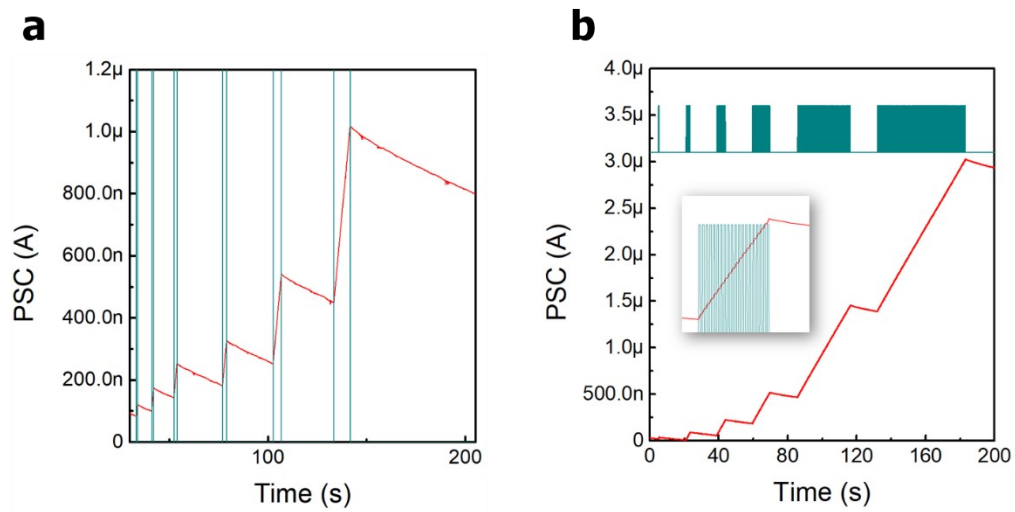## III. Measurement of optoelectronic properties.

Figure S6. (a) Spike-duration time-dependent PSC amplitude triggered by one optical spike; (b) Spike-number-dependent PSC amplitude triggered by a train of optical spikes.

IV. Au nanoparticles and FDTD simulations.

The RF module of COMSOL Multiphysics software was used to analyze the structure and calculate the strengthened electrical fields near the NPs [s1-s4]. The optical constants of Au and water were taken from the previous literature [s5]. and that of ITO was measured using a spectroscopic ellipsometer. The UV–vis absorption spectra was conducted on the AGILENT Cary 5000 UV-vis-NIR spectrophotometer.
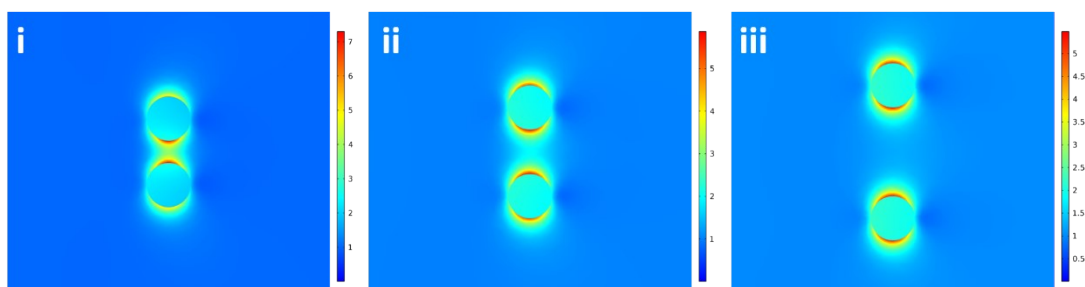

Figure S7. Surface plasmon resonance and calculated electric field distribution of Au sphere.

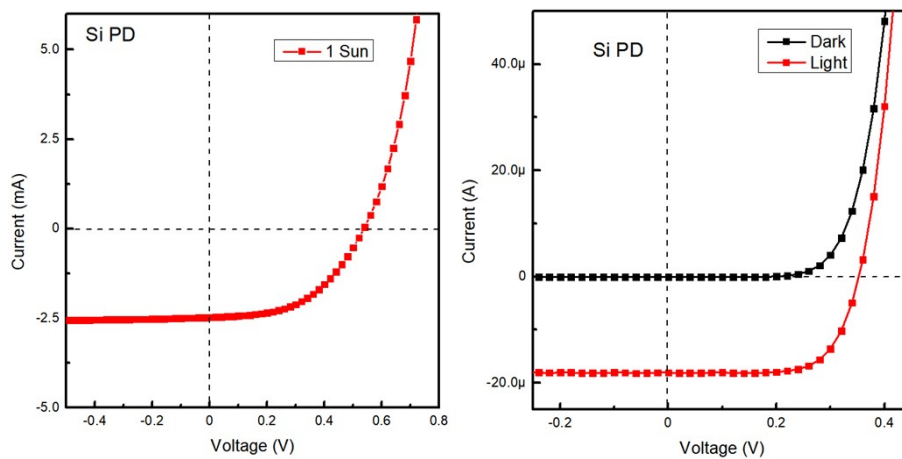# V. Construction of artificial iris vision system

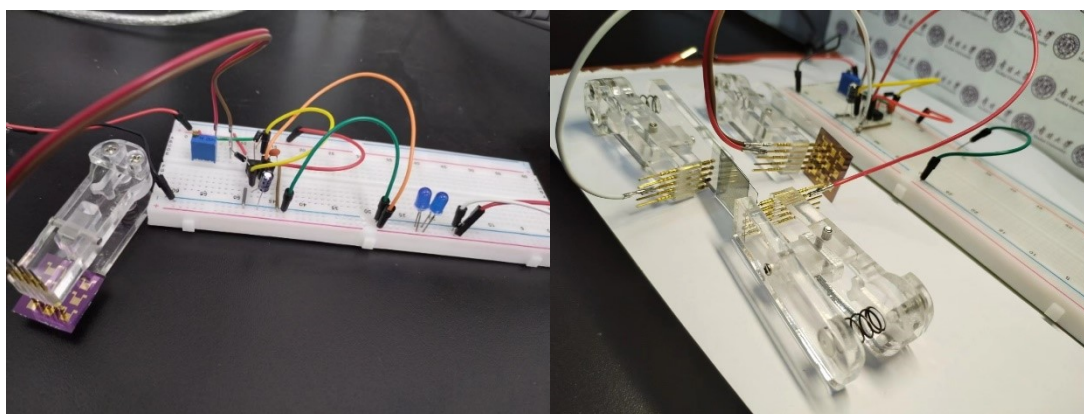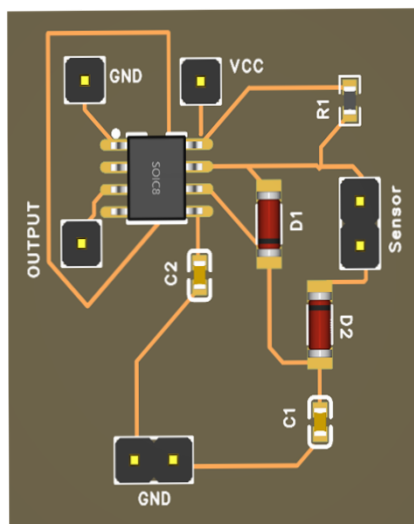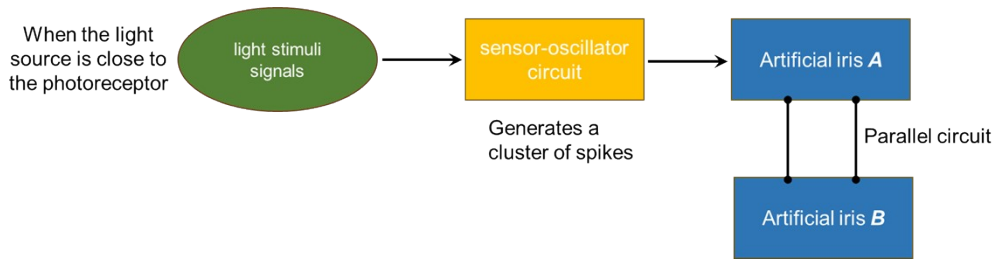Figure S8. The *I-V* characteristics of Si photodetector.

Figure S9. The photosensor-multivibrator circuit.

Figure S10 Schematic diagram of the operation of artificial iris vision for simulating direct and consistent pupillary light reflexes.

Supplementary References

[s1] COMSOL Multiphysics User's Guide, Version 5.6, http://www.comsol.com/.

[s2] Atwater HA, Polman A. Plasmonics for improved photovoltaic devices. *Nat Mater* 2010; 9: 205–213.

[s3] Amendola, V., Pilot, R., Frasconi, M., Maragò, O. M., & Iatì, M. A. Surface plasmon resonance in gold nanoparticles: a review. *J. Phys.: Condens. Matter*, 2017, 29, 203002.

[s4] Jiang RB, Li BX, Fang CH, Wang JF. Metal/semiconductor hybrid nanostructures for plasmon-enhanced applications. *Adv Mater* 2014; 26: 5274–5309.

[s5] Palik, E. D. *Handbook of Optical Constants of Solids*, 1st ed.; Academic Press: New York, 1985.